ANALYTICAL SCIENCES MAY 2017, VOL. 33

Notes

Mass Transfer in Mesoporous Microparticles Studied by Confocal Fluorescence Recovery after Photobleaching

Tatsumi SATO, Katsuya HATA, and Kiyoharu NAKATANI†

Division of Chemistry, Faculty of Pure and Applied Sciences, University of Tsukuba, 1-1-1 Tennoudai, Tsukuba, Ibaraki 305–8571, Japan

The intraparticle diffusion of a fluorescent dye in single microparticles in an aqueous solution was analyzed using fluorescence recovery after photobleaching, with a confocal fluorescence microscope. The fluorescence depth profile of single microparticles, and the fluorescence recovery at the particle center, were measured; further, the intraparticle diffusion coefficient was determined through simulations of three-dimensional diffusion in the respective microparticles. The intraparticle diffusion of coumarin 102 in octadecylsilyl silica gel was limited by the surface diffusion.

Keywords Porous material, diffusion, ODS silica gel, photobleaching, confocal fluorescence microscope

(Received November 20, 2016; Accepted February 7, 2017; Published May 10, 2017)

Introduction

The mass-transfer processes of solutes in mesoporous material/solution systems are highly influential concerning the performance of liquid chromatography,[1,2] solid-phase extraction,[3] catalyst systems,[1,4] and drug-delivery systems.[2,5] These processes consist of diffusion through the pore solution (pore diffusion), diffusion along the pore walls (surface diffusion), adsorption/desorption and chemical reactions at the pore walls, and so on;[1,6,7] further, quantitative measurements of intraparticle mass transfer rates are generally difficult to obtain. Pore and surface diffusion have been kinetically analyzed using sophisticated high-performance liquid chromatography,[8,9] microspectroscopy for single microparticles,[10–17] and so forth.[18–20] We have reported on intraparticle diffusion in silica gel and octadecylsilyl (ODS) silica gel in aqueous solutions, using microspectroscopy for single microparticles.[14–17] A single microparticle was injected into a solution, and the distribution or release rates of a solute between the microparticle and the surrounding solution phase were analyzed using microspectroscopic measurements of the single microparticle. In the silica-gel system, the mass transfer rate of rhodamine 6G (Rh6G) was limited by pore diffusion.[21,22] In the ODS silica-gel system, on the other hand, the rate-determining step of the mass transfer processes of coumarin 102 (C102) was the diffusion between the microparticle surface and the bulk solution phase (external diffusion).[23,24] However, the intraparticle diffusion of C102 in ODS silica gel was rapid, and could not be fully analyzed using the given technique. The application range of each method is limited; thus, further kinetic analysis methods will be necessary for a greater understanding of intraparticle mass transfer.

The diffusion of a fluorescent compound in biological cell systems has also been analyzed, using fluorescence recovery after photobleaching (FRAP), with a confocal fluorescence microscope.[25,26] The distribution inequilibrium of the fluorescent compound could be rapidly obtained by laser irradiation of a micrometer-sized area; the diffusion rate was then measured based on the fluorescence recovery at the irradiated area. In the present study, the FRAP method was applied, to analyze the intraparticle diffusion rate of a fluorescent dye in silica gel and ODS silica gel systems. We here discuss the potential of this approach, and the intraparticle diffusion mechanism of C102 in ODS silica gel in an aqueous solution.

Experimental

Silica gel (Kanto Chemical Co., Silica Gel 60: spherical, particle radius (r_p), 20 – 50 μm; surface area (A_s), 700 m^2 g^{-1}; pore diameter (d_p), 6.5 nm; pore volume, 1.15 cm^3 g^{-1}), ODS silica gel (Wako Pure Chemical Industries, Wakosil 40C18: spherical, r_p, 10 – 30 μm; A_s, 330 m^2 g^{-1}; d_p, 12 nm; pore volume, 1.0 cm^3 g^{-1}), Rh6G (Aldrich, 99%), and C102 (Wako Pure Chemical Industries, JIS Special Grade) were used without further purification. Water was used after deionization and distillation (Yamato Scientific, Auto Still WG203). The silica gel was soaked in water overnight.[22] Several silica-gel microparticles were injected into an aqueous Rh6G (1.0×10^{-6} mol dm^{-3}) and HCl (pH 2) solution (4 cm^3), using a microcapillary injection/manipulation system (Narishige, MN-151/IM-16), and stored for over 1 h for FRAP measurements. The ODS silica gel was soaked in an *N*,*N*-dimethylformamide (DMF, 50 vol%)–water solution, and stored for over a day. Several ODS silica-gel microparticles were injected into a DMF (0 – 5 vol%)-water solution containing C102 ($(0.2 - 2.0) \times 10^{-6}$ mol dm^{-3}) (4 cm^3), and stored over 7 days for the FRAP measurements.[23]

The intraparticle diffusion in single microparticles was measured by the FRAP method, using a confocal fluorescence microscope system (Olympus, FV-1000D). The beam of a

† To whom correspondence should be addressed.
E-mail: nakatani@chem.tsukuba.ac.jp

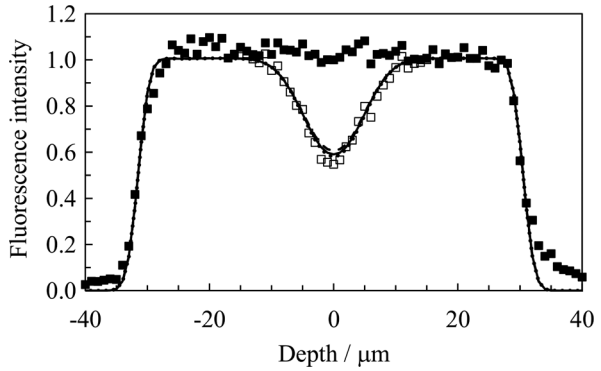

Fig. 1 Fluorescence depth profiles of Rh6G in a single silica-gel microparticle (r_p = 31.0 μm) in water before (■) and after (□) photobleaching (t = 0.4 s). The solid ($D = 5 \times 10^{-9}$ cm^2 s^{-1}), dashed ($D = 7 \times 10^{-9}$ cm^2 s^{-1}), and dotted ($D = 3 \times 10^{-9}$ cm^2 s^{-1}) curves represent the simulations using Eqs. (1) and (2), with A = 6 s^{-1} and B = 0.03 μm^{-2}.

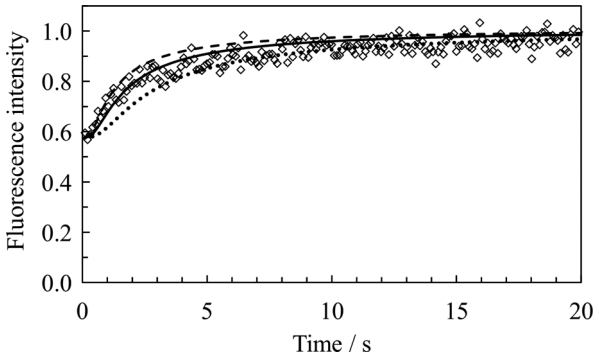

Fig. 2 Time course of the fluorescence intensity at the center of a single silica-gel microparticle (r_p = 31.0 μm) after photobleaching. The solid ($D = 5 \times 10^{-9}$ cm^2 s^{-1}), dashed ($D = 7 \times 10^{-9}$ cm^2 s^{-1}), and dotted ($D = 3 \times 10^{-9}$ cm^2 s^{-1}) curves represent the simulations using Eqs. (1) and (2), with A = 6 s^{-1} and B = 0.03 μm^{-2}.

405 nm-CW diode laser (50 mW) for C102 in ODS silica gel, and beams of 405 nm (50 mW)- and 473 nm (25 mW)-CW diode lasers for Rh6G in silica gel, were irradiated onto the center of the respective microparticles, within a circular area (1.6 μm radius) at time (t) from 0 to 0.1 s (with the lasers in tornado scan mode). After photobleaching, the microparticles were irradiated with the beam of a CW diode laser of 405 nm (0.15 mW) for C102 or 473 nm (0.45 mW) for Rh6G, and the fluorescence of 425 – 525 nm for C102 or 485 – 585 nm for Rh6G was measured from t = 0.1 s. The fluorescence depth (longitudinal (Z) axis) profile was determined based on the fluorescence intensity of a lateral (XY axes) circular (1.6 μm radius) area from the lower to upper part, along the central axis, of each microparticle. All measurements were performed at room temperature (~298 K) using an objective lens of 60-fold magnification (Olympus, UPLSAPO 60XW, NA = 1.2) and a confocal aperture of 100 μm.

The distribution coefficient and Langmuir isotherm parameters of C102 in the ODS silica gel system were determined on the basis of absorption microspectroscopy for single microparticles, and conventional absorption spectroscopy for the aqueous solution phase.[15]

Results and Discussion

FRAP in a single mesoporous microparticle

The fluorescence depth profiles of Rh6G in a single silica gel microparticle were measured at the center of the microparticle before and after photobleaching (t = 0.4 s) (Fig. 1). For kinetic analysis of intraparticle diffusion, the coordinate value of the microparticle center was defined as the origin in polar coordinates. The Rh6G was adsorbed into the silica gel microparticle interior before photobleaching. The adsorbed Rh6G molecules were efficiently bleached by high-power laser irradiation (distribution inequilibrium), and the fluorescence intensity was recovered with t. The shape of the bleached Rh6G distribution at t = 0.4 s was analogous to the Gaussian shape. The bleached Rh6G distribution depends on the photochemical reactivity of the fluorescent dye, the refractive indices of the microparticle and the solution, and so forth. Therefore, the intraparticle diffusion of Rh6G in a single silica-gel microparticle was analyzed in terms of both the fluorescence depth profile at t = 0.4 s (Fig. 1) and the t course of the fluorescence intensity (I_F) at the microparticle center (Fig. 2).

The t dependence of the fluorescent dye concentration in the microparticle ($C(r, \theta, t)$) was simulated using Eqs. (1) and (2).[6,7,14] The intraparticle diffusion rate of the dye may be changed by microscopic inhomogeneous distribution of d_p (averaged d_p = 6.5 nm for silica gel), the pore shape, and the distance between adsorption sites near to the adsorbed dye. Nonetheless, the intraparticle diffusion rate was assumed to be analyzable using a single diffusion coefficient.

$$\partial C(r, \theta, t)/\partial t = D\{(1/r^2)\partial/\partial r(r^2\partial/\partial r) + 1/(r^2\sin\theta)\partial/\partial\theta(\sin\theta\partial/\partial\theta)\}C(r, \theta, t) - A\exp\{-B(r\cos\theta)^2\}C(r, \theta, t) \quad (\text{at } 0 \text{ s} \le t \le 0.1 \text{ s and } r\sin\theta \le r_b) \quad (1)$$

$$\partial C(r, \theta, t)/\partial t = D\{(1/r^2)\partial/\partial r(r^2\partial/\partial r) + 1/(r^2\sin\theta)\partial/\partial\theta(\sin\theta\partial/\partial\theta)\}C(r, \theta, t) \quad (\text{at } 0.1 \text{ s} < t \text{ or at } 0 \text{ s} \le t \text{ and } r_b < r\sin\theta) \quad (2)$$

where r is the radially-directed spatial coordinate, θ is the polar angle between the Z and r axes, D is the diffusion coefficient of the dye in the microparticle, r_b is the radius of the photobleaching area, and A and B correspond to the parameters of photobleaching strength and width, respectively. The third term on the right side of Eq. (1) is related to the photobleaching rate, which was assumed to be a first-order reaction,[27] dependent on the incident light intensity along the Z axis. The first-order rate constant was approximated to be the Gaussian function ($A\exp\{-B(r\cos\theta)^2\}$). The initial and boundary conditions are given by $C(r, \theta, 0) = C_{eq}$ at $r \le r_p$ and $\partial C_p(0, \theta, t)/\partial r = \partial C_p(r, 0, t)/\partial\theta = \partial C_p(r, \pi, t)/\partial\theta = 0$, respectively, where C_{eq} is the dye concentration in the microparticle at the distribution equilibrium (before photobleaching). As an additional boundary condition in the Rh6G-silica gel system, $C_p(r_p, \theta, t)$ was assumed to be equal to C_{eq} because the external diffusion of Rh6G was much faster than the intraparticle diffusion.[21,22] The simulations of both the fluorescence depth profile at t = 0.4 s and I_F were performed using Eqs. (1) and (2), with the same D, A, and B values as variable parameters, under the following conditions: Δt = 1 ms, Δr = 1 μm, and $\Delta\theta = \pi/18$.

The calculated fluorescence depth profile was corrected by the spatial resolution of the confocal fluorescence microscope (spread of fluorescence from a position under the present experimental conditions, $\exp(-0.807Z^2)$).[22] The corrected

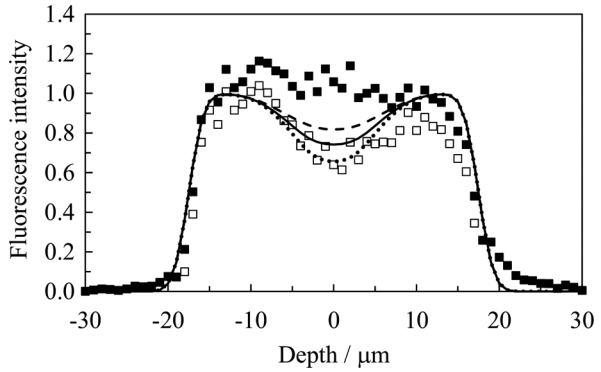

Fig. 3 Fluorescence depth profiles of C102 in a single ODS silica-gel microparticle (r_p = 16.9 μm) in water (0 vol% DMF) before (■) and after (□) photobleaching (t = 0.4 s). The solid ($D = 2.5 \times 10^{-8}$ cm^2 s^{-1}), dashed ($D = 4.0 \times 10^{-8}$ cm^2 s^{-1}), and dotted ($D = 1.5 \times 10^{-8}$ cm^2 s^{-1}) curves represent the simulations using Eqs. (1) and (2), with A = 6.8 s^{-1} and B = 0.035 μm^{-2}.

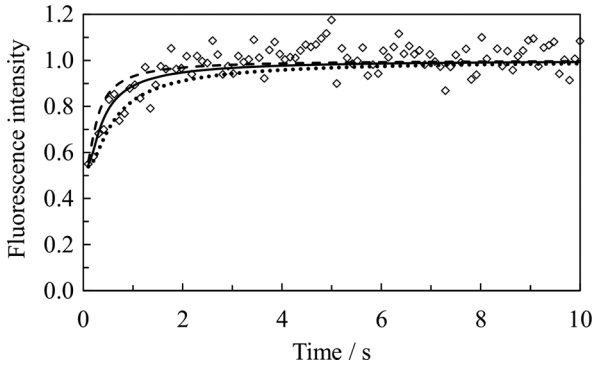

Fig. 4 Time course of fluorescence intensity at the center of a single ODS silica-gel microparticle (r_p = 16.9 μm) (0 vol% DMF) after photobleaching. The solid ($D = 2.5 \times 10^{-8}$ cm^2 s^{-1}), dashed ($D = 4.0 \times 10^{-8}$ cm^2 s^{-1}), and dotted ($D = 1.5 \times 10^{-8}$ cm^2 s^{-1}) curves represent the simulations using Eqs. (1) and (2), with A = 6.8 s^{-1} and B = 0.035 μm^{-2}.

fluorescence depth profile and I_F were compared with the observed data. The D value for the best-fitted curves in the silica-gel system was $(5.0 \pm 0.5) \times 10^{-9}$ cm^2 s^{-1} (Figs. 1 and 2), which agreed very well with that determined by the distribution rate measurements for Rh6G from water into single silica-gel microparticles.[15,22] The fluorescence-recovery curve in a biological cell system has frequently been analyzed in terms of two-dimensional diffusion.[26] When the fluorescence-recovery curve in the present study was analyzed using the two-dimensional diffusion model, the estimated diffusion coefficient was 15×10^{-9} cm^2 s^{-1}, three times greater than that determined by using Eqs. (1) and (2). Thus, for the silica gel system, three-dimensional diffusion analysis is indispensable; and the intraparticle diffusion in mesoporous microparticles was here successfully analyzed on the basis of the FRAP and three-dimensional diffusion analysis.

Pore and surface diffusion in ODS silica gel

The intraparticle diffusion of C102 in the ODS silica gel/water (0 vol% DMF) system was analyzed using the above FRAP and three-dimensional diffusion analysis, as shown in Figs. 3 and 4. As an additional boundary condition of the simulations in the C102-ODS silica gel system, $\partial C_p(r_p, \theta, t)/\partial r$ was assumed to be equal to 0 because the external diffusion of C102 was much slower than the intraparticle diffusion. The D value for C102 in the ODS silica gel/water system (2.5×10^{-8} cm^2 s^{-1}) was much greater than that for Rh6G in the silica gel system (5×10^{-9} cm^2 s^{-1}). As reported previously, in release-rate measurements for C102 from single ODS silica gel microparticles into water, the release rate of C102 was limited by the external diffusion, given by $3D_w/(r_p^2R)$, as the rate constant, where D_w is the diffusion coefficient of C102 in bulk water phase and R is the distribution coefficient of C102 between the ODS silica gel and water phases, and the intraparticle diffusion was very rapid.[23,24] That conclusion is consistent with the results of the present study.

The intraparticle diffusion of C102 in ODS silica gel was analyzed based on the pore and surface diffusion model.[4,21,28-30] In this model, D is given by

$$D = D_wH/\{\tau_p(1 + R)\} + D_sR/\{\tau_s(1 + R)\}, \quad (3)$$

where D_s is the surface diffusion coefficient. D_w was reported to be 6×10^{-6} cm^2 s^{-1}.[31] H is the hindrance parameter, dependent on the molecular diameter of C102 (a, 1.2 nm) and d_p (12 nm). Using the Renkin equation: $H = \{1 - (a/d_p)\}^2\{1 - 2.10(a/d_p) + 2.09(a/d_p)^3 - 0.95(a/d_p)^5\}$,[30] H was calculated to be 0.69. τ_p and τ_s are the tortuosity of the pore and surface diffusion, respectively; and were reported to be 1.5 – 2.3 for silica gel.[29] R was determined using $R = C_{eq}/(\varepsilon_pC_{w,eq})$,[29] where $C_{w,eq}$ and ε_p are the C102 concentration in the aqueous solution at the distribution equilibrium and the porosity of ODS silica gel (0.69),[17] respectively. The first and second terms on the right side of Eq. (3) correspond to the pore and surface diffusion terms, respectively.

Table 1 R and D of C102 in the ODS silica gel system in the absence and presence of DMF

DMF, vol%	R	D/cm^2 s^{-1}
0	$(7.5 \pm 0.9) \times 10^4$	$(2.5 \pm 0.5) \times 10^{-8}$
1	$(3.8 \pm 0.7) \times 10^4$	$(2.2 \pm 0.5) \times 10^{-8}$
5	$(8.1 \pm 0.1) \times 10^3$	$(1.8 \pm 0.5) \times 10^{-8}$

According to Eq. (3), D is a function of R. In order to confirm the R dependence of D, R was varied by the addition of small amounts of DMF to the aqueous solution. A decrease in the relative permittivity of the solution and/or an increase in the microscopic polarity of the adsoprion sites by distribution of DMF in the ODS phase will proceed by the DMF addition. Acually, R of C102 as a poorly water-soluble organic compound decreased with the increasing DMF concentration. As summarized in Table 1, R varied with the varying DMF concentration (0 – 5 vol% DMF), while the maximum fluorescence wavelength of C102 (466 – 470 nm) was almost independent of the DMF concentration. In the present system, the surface-diffusion term in Eq. (3) is approximated to D_s/τ_s, because $R >> 1$. Therefore, the slope and intercept of the D *vs.* $(1 + R)^{-1}$ plot correspond to D_wH/τ_p and D_s/τ_s, respectively. For 0 – 5 vol% DMF, the D value was independent of R, namely, $(1 + R)^{-1}$, indicating that the contribution of pore diffusion to D is negligibly small. In the Rh6G-silica gel/water system, D was directly proportional to $(1 + R)^{-1}$ without the intercept, so that the rate-determining step of the intraparticle diffusion was pore diffusion.[21,22] In the ODS silica-gel system, furthermore, the pore diffusion term is theoretically calculated to be 3×10^{-11} – 3×10^{-10} cm^2 s^{-1}, using Eq. (3). Thus, D is expected

to be governed by the surface diffusion of C102, and D_s was determined to be $(2 - 7) \times 10^{-8}$ cm^2 s^{-1} using $\tau_s = 1.5 - 2.3$.[29]

The area occupied by an adsorbed C102 molecule (S) in the ODS silica gel system was calculated to be 1.8×10^{-17} m^2, using $S = A_s/[N_A C_{p,L}/\{\rho_s(1 - \varepsilon_p)\}]$ in the absence of DMF, where ρ_s and N_A are the particle density (2.2 g cm^{-3})[29] and the Avogadro constant, respectively. $C_{p,L}$ is the saturated amount of C102 adsorbed in the microparticle and was determined to be $(2.0 \pm 0.4) \times 10^{-2}$ mol dm^{-3} from the Langmuir isotherm analysis for $C_{w,eq} = (3.55 - 107) \times 10^{-8}$ mol dm^{-3} (Langmuir isotherm constant, $(7.6 \pm 1.6) \times 10^6$ dm^3 mol^{-1}). Because the S value corresponds to a circular area of radius 2.4 nm, the distance between the centers of the adjacent adsorption sites on the pore walls is estimated to be 4.8 nm. Meanwhile, the length of an octadecyl group is 2.3 nm,[32] and a for C102 is 1.2 nm. Therefore, C102 will efficiently diffuse along the pore walls covered by the octadecyl groups, without the desorption of C102 into the pore solution (surface diffusion).[28,33,34]

Conclusions

The intraparticle diffusion of a fluorescent dye in mesoporous microparticles in solution was elucidated by the FRAP method and the three-dimensional diffusion simulations. D values less than 10^{-8} cm^2 s^{-1} could be determined by the present technique. The intraparticle diffusion of C102 in ODS silica gel was analyzed on the basis of the pore and surface diffusion model, and was governed by surface diffusion, in contrast to the intraparticle diffusion of Rh6G in silica gel (pore diffusion). The present approach has significant potential for analyzing chemical and physical processes in mesoporous particles.

Acknowledgements

The authors would like to thank the Chemical Analysis Division and Open Facility, Research Facility Center for Science and Technology, University of Tsukuba, for allowing us to use the confocal fluorescence microscope (Olympus, FV 1000-D).

References

1. D. M. Ruthven, "*Principles of Adsorption and Adsorption Processes*", **1984**, Wiley, New York.
2. N. Wu, M. A. Hubbe, O. J. Rojas, and S. Park, *BioResources*, **2009**, *4*, 1222.
3. M. C. Hennion, *J. Chromatogr. A*, **1999**, *856*, 3.
4. D. M. Ruthven, *Chem. Eng. Sci.*, **2004**, *59*, 4531.
5. S. Zhang, K. Kawakami, L. K. Shrestha, G. C. Jayakumar, J. P. Hill, and K. Ariga, *J. Phys. Chem. C*, **2015**, *119*, 7255.
6. H. Yoshida, M. Yoshikawa, and T. Kataoka, *AIChE J.*, **1994**, *40*, 2034.
7. S. A. C. Ghosh, K. Satyanarayana, R. C. Srivastava, and N. N. Dutta, *Colloid. Surf. A*, **1995**, *96*, 219.
8. K. Miyabe and M. Suzuki, *AIChE J.*, **1995**, *41*, 548.
9. R. Bujalski and F. F. Cantwell, *J. Chromatogr. A*, **2004**, *1048*, 173.
10. M. D. Ludes, S. R. Anthony, and M. J. Wirth, *Anal. Chem.*, **2003**, *75*, 3073.
11. N. Kameta, H. Minamikawa, Y. Someya, H. Yui, M. Masuda, and T. Shimizu, *Chem. Eur. J.*, **2010**, *16*, 4217.
12. H. Xu, S. Nagasaka, N. Kameta, M. Masuda, T. Ito, and D. A. Higgins, *Phys. Chem. Chem. Phys.*, **2016**, *18*, 16766.
13. H.-B. Kim, M. Hayashi, K. Nakatani, N. Kitamura, K. Sasaki, J. Hotta, and H. Masuhara, *Anal. Chem.*, **1996**, *68*, 409.
14. K. Nakatani and T. Sekine, *Langmuir*, **2000**, *16*, 9256.
15. T. Sekine and K. Nakatani, *Langmuir*, **2002**, *18*, 694.
16. K. Nakatani, M. Miyanaga, and Y. Kawasaki, *Anal. Sci.*, **2011**, *27*, 1253.
17. H. Kakizaki, C. Aonuma, and K. Nakatani, *J. Colloid Interface Sci.*, **2007**, *307*, 166.
18. F. Roncaroli and M. A. Blesa, *J. Colloid Interface Sci.*, **2011**, *356*, 227.
19. A. Yamaguchi, M. M. Mekawy, Y. Chen, S. Suzuki, K. Morita, and N. Teramae, *J. Phys. Chem. B*, **2008**, *112*, 2024.
20. R. L. Hansen and J. M. Harris, *Anal. Chem.*, **1996**, *68*, 2879.
21. T. Sekine and K. Nakatani, *Chem. Lett.*, **2004**, *33*, 600.
22. T. Sato and K. Nakatani, *Anal. Sci.*, **2017**, *33*, 179.
23. K. Nakatani and E. Matsuta, *Anal. Sci.*, **2015**, *31*, 557.
24. K. Nakatani, E. Matsuta, and Y. Kawasaki, *Bunseki Kagaku*, **2016**, *65*, 145.
25. J. C. G. Blonk, A. Don, H. van Aalst, and J. J. Birmingham, *J. Microsc.*, **1993**, *169*, 363.
26. M. Kang, C. A. Day, A. K. Kenworthy, and E. DiBenedetto, *Traffic*, **2012**, *13*, 1589.
27. C. Eggeling, J. Widengren, R. Rigler, and C. A. M. Seidel, *Anal. Chem.*, **1998**, *70*, 2651.
28. R. Bujalski and F. F. Cantwell, *Anal. Chem.*, **2006**, *78*, 1593.
29. R. Bujalski and F. F. Cantwell, *Langmuir*, **2001**, *17*, 7710.
30. W. M. Deen, *AIChE J.*, **1987**, *33*, 1409.
31. A. K. Mandal, D. K. Das, A. K. Das, S. S. Monjumdar, and K. Bhattacharyya, *J. Phys. Chem. B*, **2011**, *115*, 10456.
32. L. C. Sander, C. J. Glinka, and S. A. Wise, *Anal. Chem.*, **1990**, *62*, 1099.
33. K. Miyabe and G. Guiochon, *Anal. Chem.*, **2000**, *72*, 1475.
34. K. Miyabe, S. Sotoura, and G. Guiochon, *J. Chromatogr. A*, **2001**, *919*, 231.